



<b>Publication Year</b>	2018
<b>Acceptance in OA @INAF</b>	2020-12-29T10:24:48Z
<b>Title</b>	Status of the preliminary design of the NGS WFS subsystem of MAORY
<b>Authors</b>	BONAGLIA, MARCO; BUSONI, LORENZO; PLANTET, CEDRIC ANTOINE ADRIEN GABRIEL; AGAPITO, GUIDO; Giordano, C.; et al.
<b>DOI</b>	10.1117/12.2313266
<b>Handle</b>	<a href="http://hdl.handle.net/20.500.12386/29259">http://hdl.handle.net/20.500.12386/29259</a>
<b>Series</b>	PROCEEDINGS OF SPIE
<b>Number</b>	10703

# PROCEEDINGS OF SPIE

[SPIDigitalLibrary.org/conference-proceedings-of-spie](https://spiedigitallibrary.org/conference-proceedings-of-spie)

## Status of the preliminary design of the NGS WFS subsystem of MAORY

Bonaglia, M., Busoni, L., Plantet, C., Agapito, G., Giordano, C., et al.

M. Bonaglia, L. Busoni, C. Plantet, G. Agapito, C. Giordano, A. Puglisi, S. Esposito, G. Di Rico, A. Valentini, I. Di Antonio, M. Bellazzini, P. Ciliegi, E. Diolaiti, P. Feautrier, R. Ragazzoni, "Status of the preliminary design of the NGS WFS subsystem of MAORY," Proc. SPIE 10703, Adaptive Optics Systems VI, 107034D (17 July 2018); doi: 10.1117/12.2313266

**SPIE.**

Event: SPIE Astronomical Telescopes + Instrumentation, 2018, Austin, Texas, United States

# Status of the preliminary design of the NGS WFS subsystem of MAORY

Bonaglia M.<sup>a</sup>, Busoni L.<sup>a</sup>, Plantet C.<sup>a</sup>, Agapito G.<sup>a</sup>, Giordano C.<sup>a</sup>, Puglisi A.<sup>a</sup>, Esposito S.<sup>a</sup>, Di Rico G.<sup>b</sup>, Valentini A.<sup>b</sup>, Di Antonio I.<sup>b</sup>, Bellazzini M.<sup>c</sup>, Ciliegi P.<sup>c</sup>, Diolaiti E.<sup>c</sup>, Feautrier P.<sup>d</sup>, and Ragazzoni R.<sup>e</sup>

<sup>a</sup>Osservatorio Astrofisico di Arcetri, L.go E. Fermi 5, 50125 Firenze, Italy

<sup>b</sup>Osservatorio Astronomico d'Abruzzo, Via M. Maggini, 64100 Teramo, Italy

<sup>c</sup>Osservatorio Astronomico di Bologna, Via P. Gobetti 93/3, 40129 Bologna, Italy

<sup>d</sup>Institut de Planétologie et d'Astrophysique de Grenoble, Rue de la Piscine 414, 38400 Saint-Martin-d'Hères, France

<sup>e</sup>Osservatorio Astronomico di Padova, Vicolo dell'Osservatorio 5, 35122 Padova, Italy

## ABSTRACT

The Natural Guide Star (NGS) Wavefront Sensor (WFS) sub-system of MAORY implements 3 Low-Order and Reference (LOR) WFS needed by the Multi-Conjugate Adaptive Optics (MCAO) system. Each LOR WFS has 2 main purposes: first, to sense the fast low-order modes that are affected by atmospheric anisoplanatism and second, to de-trend the LGS measurements from the slow spatial and temporal drifts of the Sodium layer. These features require to implement 2 different WFS sharing the same NGS and optical breadboard but being respectively a  $2 \times 2$  Shack-Hartman Sensor (SHS) working at infrared wavelengths and a slow  $10 \times 10$  SHS at visible bands. The NG WFS sub-system also provides a common support plate for the 3 WFS and their control electronics and cabling.

The paper summarizes the status of the preliminary design of the LOR Module on the road to the MAORY Preliminary Design Review (PDR), focusing mainly on the description and analysis of the opto-mechanical arrangement foreseen for the NGS WFS sub-system. Performances and the design trade-offs of the NGS WFS sub-system are analyzed in a complementary paper.<sup>8</sup> First, the requirement imposed by MAORY AO system are discussed. Then the paper gives an overview of the opto-mechanical arrangement for the main components of the sub-system: the support plate, the 3 WFS units and their interfaces to the instrument rotator. In the end the paper discusses the sub-system pointing and WFE budgets derived from different analyses. The design concept for the electronic devices of the sub-system, the cabinet arrangement and the cabling scheme are given in second complementary paper.<sup>6</sup>

**Keywords:** E-ELT, multi-conjugate adaptive optics, MAORY, Shack-Hartmann wavefront sensor, natural guide star, low-order aberrations.

## 1. INTRODUCTION

MAORY is the post-focal AO instrument of the E-ELT.<sup>5</sup> It aims to implement a MCAO correction for the MICADO<sup>4</sup> near-infrared spectrograph and imager since the telescope first-light. Moreover a single-conjugate AO mode of MAORY-MICADO will be jointly developed by the 2 instruments.<sup>2</sup> MAORY is actually in the preliminary design phase and it is made by a consortium of several Italian observatories, represented by the Istituto Nazionale di Astrofisica (INAF), the Institut de Planétologie et d'Astrophysique de Grenoble (IPAG) and the European Southern Observatory (ESO). The main goals of MAORY are to provide the  $53 \times 53''$  MICADO Field of View (FoV) with a 30% Strehl Ratio (SR), evaluated in the K band, with a 50% sky-coverage and, at the same time, to allow for astrometric observation with an accuracy of  $50 \mu\text{as}$  over times scales of up to 5 years.<sup>3</sup> Being a very complex instrument, MAORY has been separated in different sub-system managed by the many consortium partners. One of those sub-systems is represented by the AO module that groups together all the key features required by the implementation of the MCAO mode of MAORY:

---

Send correspondence to Marco Bonaglia, E-mail: marco.bonaglia@inaf.it, Telephone: +39 055 2752 200

- the 6 Laser Guide Star (LGS) WFS to perform the tomographic measurement of the atmospheric turbulence,<sup>10</sup>
- the 3 NGS WFS to overcome the anisoplanatism of the atmospheric low-order modes and to de-trend the LGS measurements, alias Low-Order and Reference (LOR) WFS,
- the post-focal Deformable Mirror (DM) that, together with the E-ELT M4 mirror, will compensate for the turbulence aberrations,
- the Real-Time Computer (RTC) required to perform the matrices multiplications needed to reconstruct the vertical distribution of the turbulence aberrations relying on the WFS measurements.<sup>7</sup>

The AO Group of the Arcetri Observatory is responsible to develop the NGS WFS sub-system of MAORY. The requirements imposed to the design of the sub-system are discussed in section 2. Briefly, it will need to implement: 3 identical LOR WFS units, a common support plate (LOR Plate), the sub-system control electronics and related cabling, control software and auxiliary loops. Hereafter in the text these elements will be also called the LOR Module.

Figure 1 shows the arrangement of the LOR Module hardware on the E-ELT Nasmyth platform. The 3 LOR WFS units and their support plate will be hosted in the so-called "Green-Doughnut" (GD) volume placed on top of the MICADO cryostat and downstream of the MAORY Post Focal Relay Optics (PFRO). In this way the 3 LOR WFS will benefit of the MCAO correction, of course in a way that depends on the off-axis distance of the NGS.

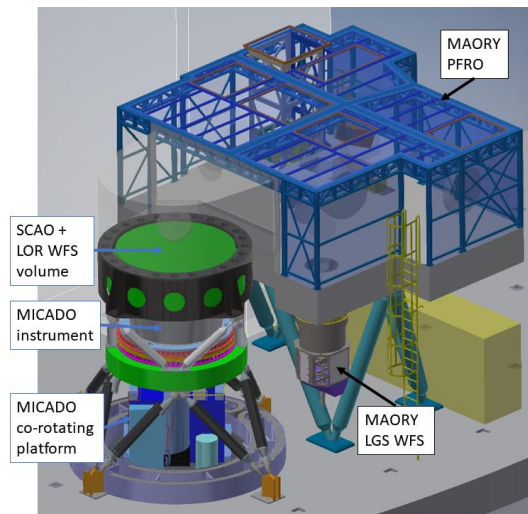


Figure 1. Sketch of MAORY and MICADO on the E-ELT Nasmyth platform. The shared volume between the SCAO and LOR WFS is highlighted in green color. The 3 LOR WFS and their support plate are rigidly connected to the instrument rotator by a support structure provided by MICADO. Most of the control electronics for the LOR Module is hosted within the 6 cabinets on the MICADO co-rotating platform.

The GD volume is sliced vertically in 2 parts on the top 400 mm height the SCAO WFS will be implemented, while on the bottom 600 mm the 3 LOR WFS will be implemented. The 3 LOR WFS units are supported by a single honeycomb steel plate (detailed in section 3.1) rigidly connected to the MICADO rotator through a support structure provided by MICADO. This scheme, represented in Figure 2, allows all the NGS WFS for field de-rotation. The LOR control electronics will be hosted within few cabinets on top of the MICADO co-rotating platform below the instrument rotator. Details on the design and arrangement of the LOR Module control electronics can be found in a complementary paper.<sup>6</sup>

The 3 LOR WFS will be arranged in a 120° geometry on their support plate. For the NGS acquisition each LOR WFS will use a couple of orthogonal stages. The patrolled field of the a LOR WFS units spans about

half of the entire technical field of 200" diameter, equivalent to an area of  $660 \times 330$  mm on the MAORY exit focal plane\*. So the FoVs of the 3 LOR WFS partially overlap to increase the number of NGS constellations accessible and hence the MCAO sky-coverage.<sup>8</sup> On top of the acquisition stages an optical breadboard will host all the LOR WFS opto-mechanics, implementing:

- a set of reflective fore-optics needed to compensate for differential effects between the 3 LOR WFS and to pre-shape the NGS beam, as detailed in section 3.2.
- A fast Low-Order (LO) WFS to sense the atmospheric tip-tilt, focus and astigmatism, directly interfaced to the MAORY RTC. This device will be described in section 3.3.
- A slow Reference (R) WFS to de-trend the LGS WFS measurements affected by the temporal and spatial instabilities of the Sodium layer, in a sort of "truth sensing" scheme.

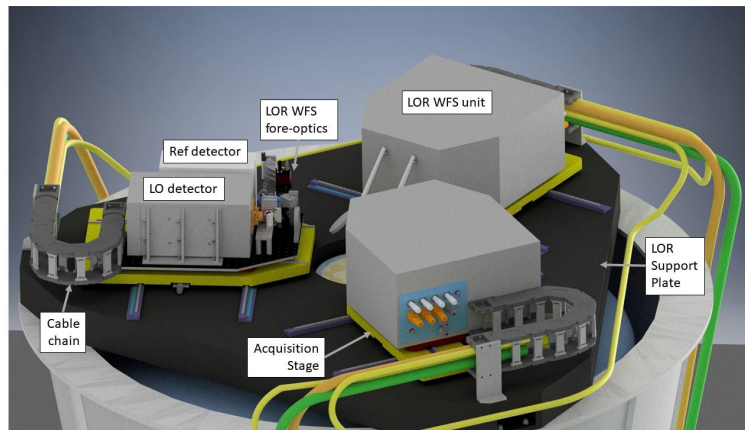


Figure 2. Sketch of the 3 LOR WFS and their support plate mounted on top of the MICADO cryostat (corresponding to the green volume shown in Figure 1). The entire sub-system is rigidly connected to the instrument rotator to provide field de-rotation to the WFS. The 3 LOR WFS units are identical and they are moving within the technical FoV by XY stages. Each optical breadboard mounted on the stages will implement both a Low-Order and a Reference WFS, plus several reflective optics needed to pre-shape the NGS beam.

The contribution of the LOR Module elements to the budgets of the AO system is analyzed in section 4, particularly the 2 most critical ones: the LOR WFS pointing error affecting the astrometric performance and its internal WFE that contributes to the MAORY non-common path aberrations with MICADO.

Finally section 5 explores the possibility to provide the LO WFS with an enhanced wavefront correction along its line-of-sight to boost the WFS sensitivity. This design option will require to re-arrange the LO WFS optical design to make room for an additional DM, while keeping untouched the R WFS and fore-optics layouts.

## 2. SUMMARY OF TECHNICAL SPECIFICATIONS

The MAORY Adaptive Optics system groups together all the key features required by the functioning of the AO module: NGS and LGS WFS, post-focal DM and the RTC. This allowed for a balanced distribution of the system error budgets and a better control of the AO and astrometric performance required to MAORY. In this framework the MAORY AO system puts tight requirements on the design of the NGS WFS sub-system, specifically:

1. To implement 3 LO WFS, being  $2 \times 2$  Shack-Hartmann sensors (SHS) to measure atmospheric tip-tilt, focus and astigmatism with a frame rate of  $100 \div 1000$  Hz and a FoV  $> 1''$ . This is a trade-off between the need to sense the low-order modes with NGS and the limiting magnitude fixed by the sky-coverage requirement ( $mag_R = 24$ ).

\*the MAORY exit focal plane reproduces the E-ELT F17.7 beam, with a 3.3 mm/" plate scale.

2. To implement 3 R WFS, being  $10 \times 10$  SHS working at  $0.1 \div 10$  Hz with a FoV  $> 2''$ . This is required to de-trend the LGS measurements affected by Sodium layer temporal and spatial instabilities. In this way the 3 R WFS are implementing a tomographic "truth sensor" able to disentangle the distribution in height of the LGS non-common path aberrations (NCPA) and to properly offset the reference slopes of the 6 LGS WFS.
3. To pickup the NGS within a technical FoV of  $200''$  diameter by the use of motorized acquisition stages supported by the MICADO de-rotator ensuring a pointing repeatability of  $6\mu\text{m}$  (equivalent to  $1.8$  mas on-sky). Obviously the FoV dimension is fixed by the sky-coverage requirement while the pointing repeatability is the result of the MAORY astrometric error budget allocation.
4. The LO and R WFS must share the same NGS and acquisition stages, hence the LO WFS is working in H band maximizing the WFS sensitivity obtained by the AO corrected PSF, while the R WFS is working in the R+I bands in partial-AO correction regime.
5. The internal wavefront error budget of the LO and R WFS must be less than  $50$  nm rms to not saturate the 2 WFS slopes when the NCPA correction with MICADO is applied.
6. The 3 LOR WFS must be able to compensate for differential focus between them with a range up to  $20$  mm and a resolution better than  $50\mu\text{m}$ . This requirement is also imposed by the need of NCPA correction.
7. Even if installed on a gravity-invariant focal station, the LOR WFS must work at Zenith angles of  $(1.5 \div 70)^\circ$ , dealing with both atmospheric chromatic dispersion and differential refraction.
8. Due to the lack of information about the final pointing error of the E-ELT, the LOR WFS must implement an acquisition camera able to find a  $mag_R = 24$  NGS with  $0.5''$  accuracy within a  $5''$  FoV in less than  $1$  s of exposure.

The technical solutions found to accomplish the design of the NGS WFS sub-system of MAORY are discussed in the next section.

### 3. DESIGN AND ANALYSIS OF THE LOR MODULE

The LOR Module hardware can be separated in 3 main units:

1. the LOR Plate that supports the 3 LOR WFS units and it acts as interface to the MICADO de-rotator,
2. the LOR WFS units, including acquisition stages, opto-mechanics and motorized components,
3. the control electronics, the electronic cabinets and cabling.

The first 2 points will be detailed in the next sections while the design concept for the last point is given in a complementary paper.<sup>6</sup>

#### 3.1 The LOR Plate

The LOR Plate is made out of a steel honeycomb structure. Its top plate is  $6$  mm thick and the bottom one is  $4$  mm thick. The distance between the 2 plates is  $150$  mm. The total mass of the plate is about  $400$  kg. The interface between the 3 LOR WFS units and the plate is represented by the longer-axis rails of the acquisition stages. Indeed, those rails will be directly welded to the plate in correspondence of the vertical stiffening structures as shown in Figure 3. The interface between the plate and the support structure connected to the instrument rotator is represented by 3 interface pods placed in correspondence of the stiffening elements of the honeycomb.

The behavior of the LOR Plate has been analyzed through FEA simulations both in static and dynamic conditions. Because of the tight requirement on the plate stiffness it has been necessary to carefully distribute the 3 LOR WFS payloads to obtain a realistic simulation of the plate behavior. Three  $100$  kg masses (corresponding

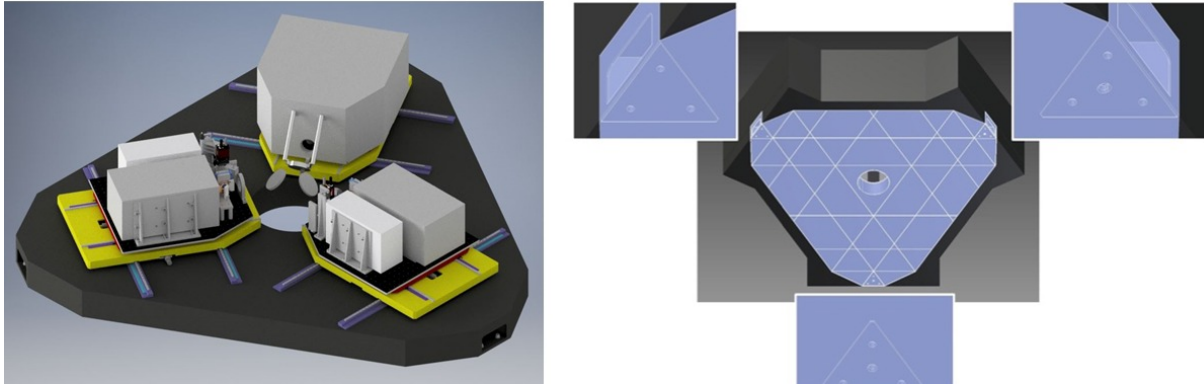


Figure 3. Left: image of the LOR Plate supporting the 3 LOR WFS and their acquisition stages. The longer-axis of the stages will be directly welded to the honeycomb structure of the plate saving vertical space and mass. Right: detail of the plate internal rib geometry and its interface pads to the MICADO support structure.

to the LOR WFS expected weight) have been applied in compression on the longer-axis rails embedded in the plate. Each mass has been applied on 4 small areas (approximately  $25 \times 50 \text{ mm}$ ) to simulate for the effect of the rail carriers supporting the LOR WFS board.

The static analysis shows the deformation of the LOR Plate when the payload of the 3 LOR WFS move along the rails. The 3 payloads have been offsetted by 60 mm, simulating for a  $10''$  dither on-sky, one after another in the 2 axes directions. Differential flexures between the 3 LOR WFS have been evaluated keeping a reference WFS in its nominal position. The static analysis confirmed the critical error to be pitch and yaw of the LOR WFS boards. Indeed, the maximum position error was  $< 0.5 \mu\text{m}$  while the maximum pitch and yaw error reached  $0.45''$ . Such a tilt of the entire LOR WFS board has an optical effect because of the differential incidence angle on the first pickoff mirror that creates a pointing error. The distance between the pickoff mirror and the focal plane is  $\sim 500 \text{ mm}$  corresponding to a pointing error of  $1 \mu\text{m}$  ( $= 0.33 \text{ mas on-sky}$ ). Summarizing, during an observation operating dithers of 10 the expected pointing error caused by the displacement of the load on the LOR Plate is  $< 0.5 \text{ mas}$  (considering correlated the shift and pitch/yaw of the LOR WFS board).

The dynamic behavior of the LOR WFS support bench has been analyzed through FEA stress simulation. The first 3 eigenfrequencies reach 96, 154 and 155 Hz respectively as shown in Figure 4.

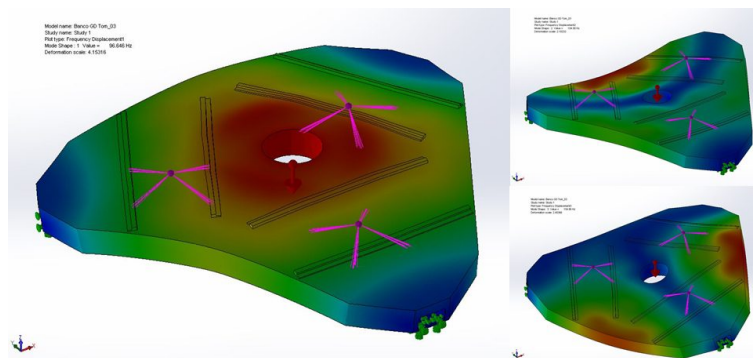


Figure 4. Results of the FEA dynamical analysis the first eigenfrequency is about 100 Hz. The pink pyramids show the load distribution considered in the analysis: a mass of 100 kg is distributed in compression on 4 small pads along the longer-axis rails. These masses have been translated by about 60 mm in the static analysis.

### 3.2 NGS pickoff and LOR WFS fore-optics

The baseline for the design of the LOR Module is to have 3 identical LOR WFS units disposed at 120° geometry around the MICADO FoV. Figure 5 schematizes the NGS pickoff scheme and the portion of the focal plane patrolled by a single LOR WFS unit. Its patrol FoV is a semi-circle with 100" radius (gray area in Figure) centered on the 53 × 53" square FoV of MICADO (yellow square in Figure). A couple of orthogonal linear stages displace the LOR WFS within a 660 × 330 mm area to effectively cover the full patrol FoV. A 45° AOI pickoff mirror, at 520 mm distance from the MAORY exit focal plane, folds the NGS beam in a plane parallel to the LOR Plate and MICADO rotator planes. The whole LOR WFS opto-mechanics is mounted on an optical breadboard of 650 × 600 mm area supported by the acquisition stages top plate.

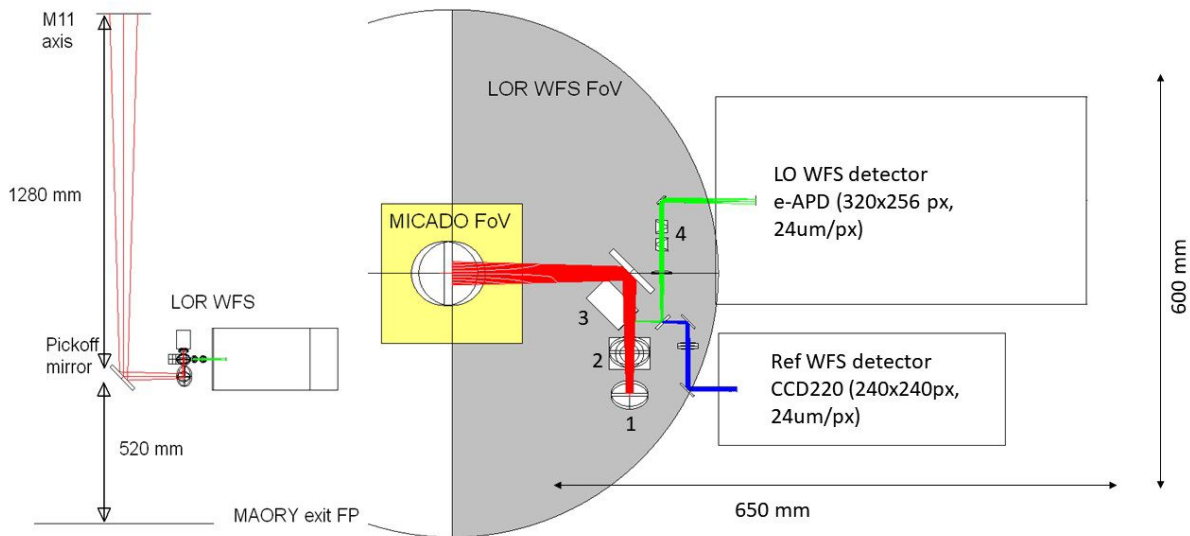


Figure 5. Scheme of the pickoff of a NGS on-axis (left) and optical layout of the LOR WFS as seen from top (right). The yellow area highlights the MICADO FoV of 53 × 53", the gray one the LOR WFS technical FoV of 200" diameter. The red color highlights the optical path in common between the LO and R WFS. The green color highlights the LO WFS optical path while the blue color the R WFS one. Hardware details are given in text.

On the front part of the breadboard the LO and R WFS share a group of fore-optics, in detail:

1. A reflective trombone to compensate for the differential longitudinal focus between the 3 LOR WFS units. The actuator is a Micronix PPS-28SM linear stage, ensuring a ±10 mm travel range with a typical accuracy of 10 μm, that's sufficient to fulfill requirement 6 of section 2.
2. A visible acquisition camera with 10" FoV. The detector chosen is a Allied/AVT GE 2040 CCD camera. A 4× field compressing lens has been designed to squeeze the acquisition camera FoV within the 15 × 15 mm active area of the detector. This device has been provided to fulfill the requirement 8 of section 2.
3. A tip-tilt mirror placed very close (± 10 mm) to the LOR WFS internal focal plane. This device will be actuated through a Physik Instrumente S335 piezo-head to adjust the pupil position on the LO and R WFS, ensuring a 50% of pupil diameter adjustment with an accuracy equivalent to 0.6 μas on-sky. The pupil steering mirror will be controlled by an auxiliary loop that measures the pupil position relying on the R WFS illumination patten. This algorithm demonstated to be able to stabilize the pupil position at the level of 0.1 sub-aperture and it is actually implemented in the LGS WFS system of ARGOS at the LBT.<sup>1</sup>



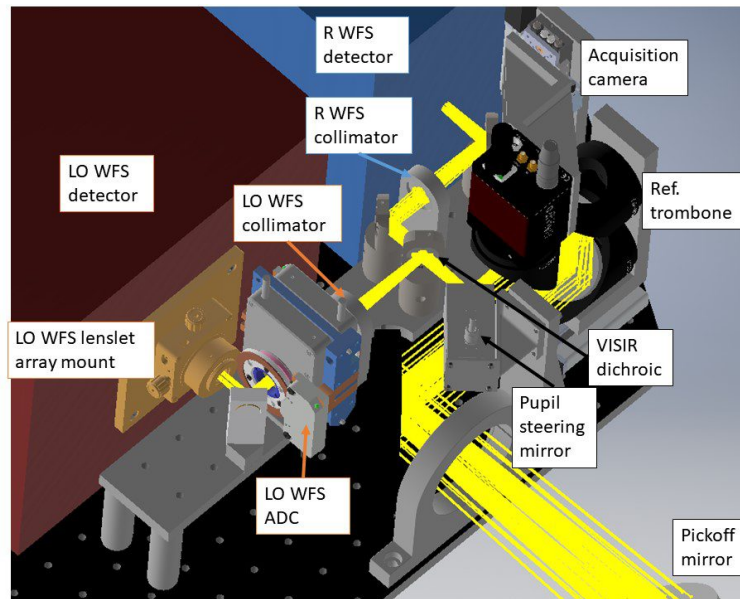


Figure 6. Sketch of the opto-mechanical component of the LO (red) and R (blue) WFS. The WFS fore-optics are also highlighted in black.

4. An infrared ADC (serving only the LO WFS). This device will compensate for the atmospheric chromatic dispersion in the H band, restoring the PSF quality on the WFS detector. The ADC optical design has been optimized to minimize the induced PSF wobble hence the LO WFS pointing error. The ADC prisms are counter rotated by two Standa 8MPR16-1 rotatory stages provided with ES5001 SSI encoder. This device has been provided to fulfill the requirement 7 of section 2.

### 3.3 Low-Order and Reference WFS

The LO and R WFS share the same light path up to a visible-infrared (VISIR) dichroic placed at  $45^\circ$  AOI  $\sim 50$  mm after the internal F17.7 focal plane. The dichroic is a 1" fused silica window that reflects the wavelengths  $> 1.1 \mu\text{m}$  towards the LO WFS and it transmits wavelengths  $< 1.1 \mu\text{m}$  to the R WFS.

The layout of the 2 WFS is similar: both optical systems produce a 5.76 mm diameter pupil through a refractive collimator of 102 mm focal length. The pupil images are sliced by a  $2 \times 2$  lens array on the LO WFS and by  $10 \times 10$  micro-lenses on the R WFS. In addition, the LO WFS makes use of an ADC to take advantage of the partially corrected PSF at infrared wavelengths. In the preliminary optical design of the LOR WFS the 2 detectors, that will be provided by ESO, have been simply considered to be arrays of  $240 \times 240$  pixels with  $24 \mu\text{m}/\text{px}$  size. In the LO WFS this allows to sample each subaperture with  $100 \times 100$  px and, considering a minimum 1" FoV, it allows for a 10 mas/px resolution through a 87 mm focal length lenses array. The R WFS will sample each subaperture with  $24 \times 24$  px. Imaging a 2" FoV onto 24 px will allow for a  $\sim 80$  mas/px scale by using a lenslet array with 8.8 mm focal length. Due to short focal length the R WFS lenslet array must be mounted inside the visible detector housing. Figure 6 shows the opto-mechanical arrangement of the 2 WFS.

## 4. BUDGETS ALLOCATION

The LOR Module engineering required for several iterations in the budgets allocations. This section focuses on the most critical ones: the total pointing error of the LO WFS, hence the position repeatability of the WFS that will impact the astrometric accuracy reachable by MAORY, and the internal wavefront error (WFE) of the LOR WFS that will increase the range of the the non-common path aberrations correction applied to the LO and R WFS, hence decreasing their dynamical ranges.

## 4.1 Pointing error

A critical requirement for the LOR Module comes from the astrometric accuracy that MAORY must be capable of reaching. The instrument top level requirement is to ensure  $50 \mu\text{as}$  accuracy in timescales from 1 hour to 5 years.<sup>9</sup> This requirement is broken down at system level and it has been translated into a specification on the opto-mechanical stability of the LOR WFS, that must be capable of keeping their relative positions with 1.8 mas stdev accuracy (corresponding to  $6 \mu\text{m}$  at the F17.7 exit focal plane of MAORY).<sup>3</sup> In fact, a displacement of a LOR WFS unit is seen as a local tilt by the AO control loop and it will compensate for it through the DMs, possibly introducing a geometric distortion on the scientific field.

The field distortion introduced on MICADO depends on the direction and sign of the tilt of the 3 LOR WFS units, e.g. consider 2 trivial cases: a rigid shift of the 3 LOR WFS units and a radial shift of each LOR WFS (equivalent to move away from the telescope optical axis each LOR WFS by the same amount). When the AO loop is closed, the first case will result in a "panning" of the field on the MICADO detector (as it will be in a dithered image), while second case it will result in a plate-scale change, hence a geometric distortion of the MICADO image. The interpretation of this specification requires to analyze any possible cause that will displace the NGS image on the LO WFS, hence introducing a pointing error. Several sources have been identified: a class of them is related to the mechanical flexures and repeatability of the LOR Plate and of the LOR WFS unit acquisition stages, another class is related to the optical properties of the PFR0 that produces a non-axisymmetric field distortion in the LOR input focal plane. Table 1 summarizes the main error sources identified and it allocates a specific budget for each contributor. Numbers have been obtained through numerical, Zemax and finite element analyses.

Table 1. Summary of the main pointing error sources in the LO WFS. The effects of the main error sources have been quantified through numerical, Zemax or thermal analysis. Numbers are in mas rms, the square sum of the error sources amounts to 1.8 mas rms.

Error source	Error [mas rms]	Notes
Field distortion from PFR0	0.5	For 5 min exposure, with 70% lookup table correction
Chief ray tilt compensation residual	0.006	Actuator accuracy (see section 3.2)
Flexures of LOR Plate	0.5	FEA result, $10''$ dithering applied (see section 3.1)
Thermal effect on LOR Plate	0.05	$\Delta T = 0.45^\circ\text{C}$ , 5 min at maximum air temperature gradient ( $\pm 1.5^\circ\text{C/h}$ )
Acquisition stages repeatability (XY plane)	0.15	Vendor technical specifications
Acquisition stages repeatability (pitch/yaw)	0.7	Vendor technical specifications
Differential focus stage	0.1	Allocated, expected from alignment residual
ADC pointing error	0.12	From Zemax analysis, see section 3.2
Contingency, alignment, thermal effects on opto-mechs	1.5	Allocated
<b>Total</b>	<b>1.8</b>	Quadrature sum

## 4.2 Internal wavefront error

Manufacturing and alignment errors of the LOR WFS optical components contribute to the NCPA budget with MICADO. The LOR Module requirements allocate 50 nm rms as maximum WFE for the LO and R WFS (see requirement 5 of section 2). The reflective fore-optics of the LOR WFS are all made of large ( $> 50 \text{ mm}$  diameter) flat mirrors at  $45^\circ$  AOI. They are in common path between the 2 WFS. The VISIR dichroic is seen in transmission by the R WFS and in reflection by the LO WFS. Both WFS are composed by refractive collimators (doublet in the R WFS, singlet in the LO WFS) and a set of small ( $< 25 \text{ mm}$  diameter) fold mirrors at  $45^\circ$  AOI. Standard

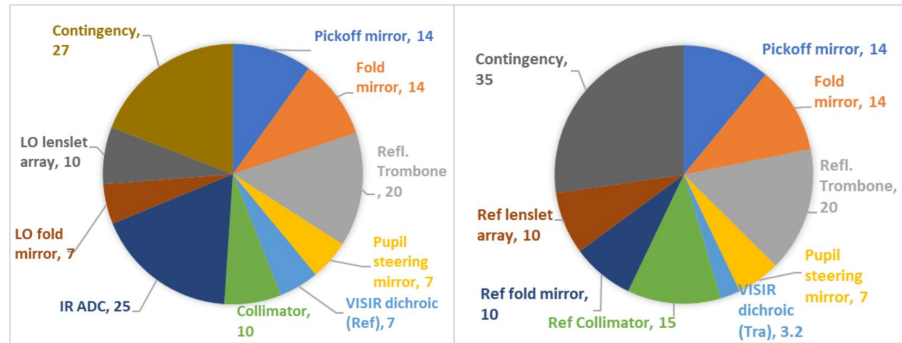


Figure 7. WFE budget allocation for the LO (left) and R (right) WFS. Numbers are in nm rms, the quadrature sum of all the contributors amounts to 50 nm rms.

WFE have been allocated to the LOR WFS optics, to account for polishing errors and possible bending due to coating. The WFE allocation varies between mirrors, lenses and prisms (e.g. ADC):

- Mirrors: large fore-optics have been specified to 10 nm rms surface error. Considering a 45° AOI it turns to a contribution of 14 nm rms WFE per reflective surface. Small WFS optics have been allocated for half of that.
- Lenses: it has been assumed that WFS collimators (LO singlet and R doublet) are polished to contribute with 10 and 15 nm WFE respectively. Other 10 nm rms WFE have been allocated to the lenslet arrays (singlets). These numbers already take into account for the air-glass interfaces and cementing contribution (doublet case).
- ADC: a total WFE of 25 nm rms have been allocated to the 2 identical prisms (ABA configuration) seen in transmission by the LO WFS. This number should account for a total of 4 air-glass surfaces, 4 glass-glass surface and the respective cementing.

Figure 7 visualizes the WFE budget allocation described above, the square sum for the total optical path for the 2 WFS are:

- LO WFS: 41.9 nm rms allowing for a contingency of about 27 nm rms,
- R WFS: 35.6 nm rms allowing for a contingency of about 35 nm rms.

## 5. DUAL ADAPTIVE OPTICS LAYOUT

The first end-to-end simulations of the complete MCAO system have shown that the correction achievable in H band might be very low ( $SR_H < 5\%$ ) on the NGS within the technical FoV. This will lead to a poor performance of the LO WFS. In order to mitigate this issue, a possible solution would be to add a dedicated DM in the optical path of each LO WFS. Controlling the DM in open loop, relying on the tomographic measurement of the atmosphere obtained through the LGS WFS measurements, it will be possible to enhance the AO correction achieved in the direction of the NGS, in a sort of Dual Adaptive Optics (DAO) scheme. This solution will require to re-arrange the LO WFS optical design to make room for an additional deformable mirror, while keeping untouched the R WFS and fore-optics layout. Figure 8 shows a possible solution for the DAO option, the main design changes in the LO WFS can be summarized in few points:

1. The IR collimator focal length increased to 150 mm, producing a ~9 mm collimated beam.
2. The IR ADC position shifted along the collimated beam to minimize the mount collision with the surrounding opto-mechanics.

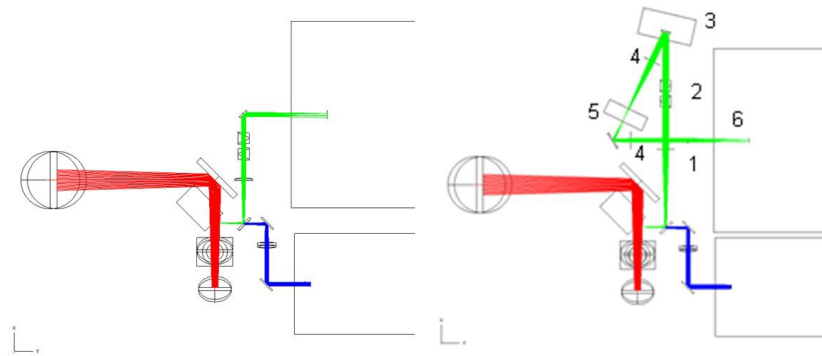


Figure 8. Comparison of the optical layout of the LOR WFS in the baseline design (left) and in the DAO option (right). Hardware details are give in the text.

3. The DM selected is a MEMS 492-3.5 produced by Boston Micromachines working at 13° AOI.
4. Two relay lenses (respectively of 90 and 60 mm focal length) are used to compress the beam to a 5.7 mm diameter as required by the SH WFS sampling.
5. A variable iris is placed in the LO WFS internal focal plane to modify the WFS FoV. The beam is a F10.4 so here the telescope plate scale is converted to 2 mm/".
6. The IR lenslet array and detector are the same of the baseline design shown in section 3.3.

## 6. CONCLUSIONS

The design of the MAORY NGS WFS sub-system is moving forward the level required by the project PDR foreseen in 2019. The main technical specification imposed by the MAORY AO system have been summarized and discussed. The overall design of the LOR Module has been presented in the paper, with a detailed insight of the opto-mechanical arrangement of the 3 LOR WFS and their support plate. The design presented fulfills the technical specifications. Finally the error sources to the LO WFS pointing error have been identified and the total budget has been broke down to them. Also the internal WFE budget of the LO and R WFS have been distributed between the optical components showing a consistent margin in the optics specification.

## REFERENCES

- [1] Bonaglia, M., et al., "Laboratory characterization of the ARGOS laser wavefront sensor", *Proc. SPIE* **8447**, article id. 84476B, 11 pp. (2012).
- [2] Clénet, Y., et al., "MICADO-MAORY SCAO: towards the preliminary design review", *Proc. SPIE* **10703-40**, (2018).
- [3] Cortecchia, F., et al., "MAORY requirements flow down and technical budgets", *Proc. SPIE* **10703-265**, (2018).
- [4] Davies, R., et al., "The MICADO first light imager for ELT: overview and operation", *Proc. SPIE* **10702-64**, (2018).
- [5] Diolaiti, E., et al., "MAORY for ELT: preliminary design overview", *Proc. SPIE* **10703-38**, (2018).
- [6] Di Rico, G., et al., "Electronics design of the NGS WFS subsystem of MAORY", *Proc. SPIE* **10703-130**, (2018).

- [7] Foppiani, I., et al., "MAORY real time computer preliminary design", *Proc. SPIE* **10703-153**, (2018).
- [8] Plantet, C., et al., "Performance analysis of the NGS WFS of MAORY", *Proc. SPIE* **10703-156**, (2018).
- [9] Pott, J. U., et al., "The MICADO first light imager for ELT: its astrometric performance", *Proc. SPIE* **10702-239**, (2018).
- [10] Schreiber, L., et al., "The MAORY laser guide star wavefront sensor: design status", *Proc. SPIE* **10703-71**, (2018).